Reactive and Active Power Control of Grid WECS Based on DFIG and Energy Storage System under both Balanced and Unbalanced Grid Conditions

Neda Azizi, Hassan Moradi CheshmehBeigi*

Department of Electrical Engineering, Faculty of Engineering, Razi University, Kermanshah, Iran.

A B S T R A C T

This paper focuses on improving the active and reactive power control of Wind Energy Conversion System (WECS) by employing the Battery Energy Storage System (BESS) and controlling the frequency and voltage regulation instantaneously. The proposed power control scheme is composed of two control loops so that they are implemented and designed for active power control and controlling the reactive power, respectively, which both are equipped with PI type controllers. In addition, two control loops were utilized to control the frequency and voltage on the rotor side converter under balance and unbalance grid conditions. In this paper, the presented control strategy optimally tuned all the parameters of controllers at the same time by utilizing a mixed integer nonlinear optimization programming and solved by the ICA algorithm. Moreover, in order to demonstrate the effectiveness of the proposed strategy, non-linear time domain simulations were carried out in MATLAB software. The obtained simulation results verified that the proposed control scheme efficiently utilize BESS to control the active and reactive power control and confirm the effectiveness of the proposed strategy under the balanced and unbalanced grid conditions.

1. INTRODUCTION

Currently, due to the problems associated with environmental degradation by conventional energy sources and the advantages of renewable energy, using this type of energy has been considered as affordable energy purposes [1]. The literature review showed that several types of electric generators have been used in WECSs as distributed generators in microgrid including squired-cage induction generator, synchronous generator with external field excitation and Doubly Fed Induction Generator (DFIG) [2-4]. Smooth operation and control of power electronic converters are essential to ensure WECSs in compliance with modern grid codes [5].

It is clear that frequency stability is vital for the operation stability of the power system [6],[7]. In order to reduce frequency oscillations in the network, there is an increasing need for regulation from variable speed wind turbines [8]. DFIG is commonly used for this purpose for electricity generation through wind energy because of the priority of its advantages than shortcomings [9]. In variable speed operation, for the wind turbine based DFIG, with active and reactive power control abilities, power losses are reduced as

compared to the wind turbine using the fixed speed generator [10]. Today, using DFIG is constantly increasing due to the flexible control of the active and reactive power established upon the Back to Back converter and active control between the induction machine and power grid [11-13].

The WECSs based on the DFIG supply huge wind energy market because of its light weight, small size, and cost-effectiveness of the generator as well as the relatively small and economic power converter [14], [15]. One way to improve the frequency regulation is the presence of the grid frequency variable and frequency deviation signal behind the nominal value in the control of rotor side converter [16-18]. Moreover, the synchronous control is another way which has been investigated in [19], [20]. Two remarkable problems encountered by the DFIG are weak low voltage ride-through ability and unstable output power. Many techniques to solve this problem have been scrutinized in the literature which can generally be classified into 1-software [21] and 2-hardware solutions [22]. A crowbar circuit is the most popular hardware solution to solve this problem [23], [24]. In [25] a new active and reactive power controller presented for on-grid BESS under unbalance condition, it tuned by the CPCE algorithm. In [26] new multiband stabilizers for

---

damping, oscillation have been presented. A novel damping control strategy for DFIG is proposed in [27].

To efficiently address the unbalanced grid voltage requirement in the converter controller of a DFIG, an additional function implement was added to the main control algorithm [28].

This paper addresses a new control strategy for controlling the active and reactive power of WECS by employing the BESS with frequency control and voltage regulation ability at the same time. The proposed control strategy can control the active and reactive power, frequency and voltage simultaneously under both balance and unbalance conditions by employing BESS. At first, the proposed control strategy calculates the sequence components of the voltage and then it utilizes positive sequence to compute the power as an input signal of the active and reactive power controllers. In addition, BESS can supply demand power of the load, if DFIG cannot supply this power or it operates in islanded mode. This paper proposes the decoupled controllers for the active and reactive power control of DFIG associate with the active and reactive power of the grid. Simulation result verified that under any fault or disturbance, the controller can command the frequency, voltage and active- reactive power of the BESS. Finally, all parameters of controllers are tuned by the ICA intelligent algorithm. Briefly, the main contributions of the current work can be highlighted as follows:

• The proposed structure regulates the voltage, controls the frequency, and enhances the active and reactive power control at the same time in the standalone and

on-grid DFIG under the balance and unbalance network conditions.

• All the parameters of the controller (voltage, frequency, active power and reactive power controllers) are tuned at the same time by the ICA algorithm. This is also one of the main contributions of the paper because all the controllers are simultaneously tuned to find the most optimal operating condition of the network. The proposed methodology results in the best operation for the whole system including BESS, DFIG, and load.

In order to deal with the real conditions, the real models of DFIG and converter are derived and simulated. The real world modeling and nonlinear time-domain simulations are carried out in MATLAB simulation software.

2. UNDERSTUDY NETWORK

Single line diagram of the understudy system is shown in Fig. 1. It can be seen that the BESS and DFIG are connected to the network at bus 2 as the case study. DFIG has two conventional voltage source converters named as rotor and grid side converter (RSC and GSC), also, a common DC-link. As shown in Fig. 1, the RSC convert the uncontrollable AC voltage to the DC one and GSC prevents the DC voltage to the controllable AC one.

It is worthy to mention that this system only opts as an illustrative test case and the proposed strategy can also be simulated on the other test system with different structures.
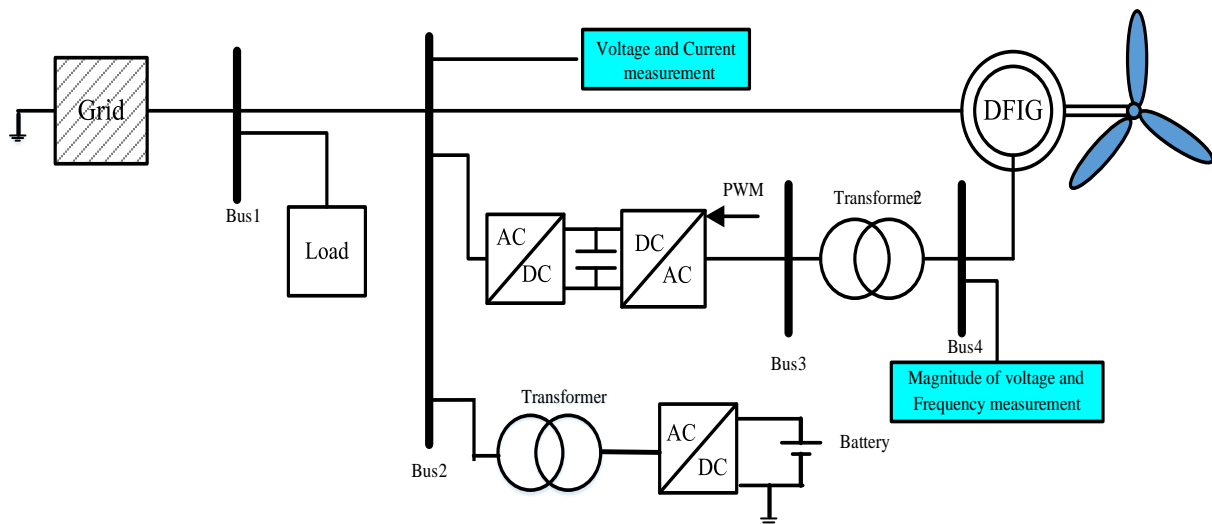

Figure 1. Structure of the understudy model.

2.1. Proposed control strategy

In order to complete the control loops of the used inverter, three-phase currents and voltages are measured and transferred to dq0 frame. Then, two control loops

are designed to decouple the control of the frequency and voltage regulation on d and q axis. Each loop is mobilized with an internal PI controller. Internal controllers are used to set the frequency and voltage on the reference values. Finally, the output dq0 signals are

transferred back to abc frame to produce an appropriate PWM signal. Because of the unbalance condition, a sequence analyzer is used to analyze the sequence of the grid voltage. Then, the negative sequence is sent to its specific control block to be eliminated and positive sequence used in the frequency and voltage controllers. Proposed strategy is revealed in Fig. 2. The configuration of the proposed controller for the active and reactive power of BESS which is injected power to the grid is shown in Fig. 3. When the system is under the unbalanced condition, negative sequence components will be present. Consequently, with an additional lock loop control system, the negative sequence voltage adjusts to zero. Therefore, DFIG and BESS will provide the power of the load together, while, DFIG operate under islanding mode, the BESS can supply the load alone. Incredibly to say that this strategy and the proposed design follow the targets in the unbalance grid condition correctly. As shown in Fig. 2, the input signal of the frequency and voltage controller of the rotor is a positive sequence of each value. As it seems in (1) and (2), v_d and v_q are calculated from the frequency and voltage signals, also, active and reactive power are calculated from (3) and (4), respectively [11]. Test parameters of the system including parameters of a wind turbine, loads and grid are summarized in Table 1.

$$\int (f - f_r)dt = v_d \qquad (1)$$

$$\int (v^- - v_r^-)dt + \int (v^+ - v_r^+)dt = v_q \qquad (2)$$

$$P = 0.5(\int (v_d^- - v_{dr}^-)dt + v_d^+)i_d + (\int (v_q^- - v_{qr}^-)dt + v_q^+)i_q \qquad (3)$$

$$Q = -0.5(\int (v_d^- - v_{dr}^-)dt + v_d^+)i_q + (\int (v_q^- - v_{qr}^-)dt + v_q^+)i_d \qquad (4)$$
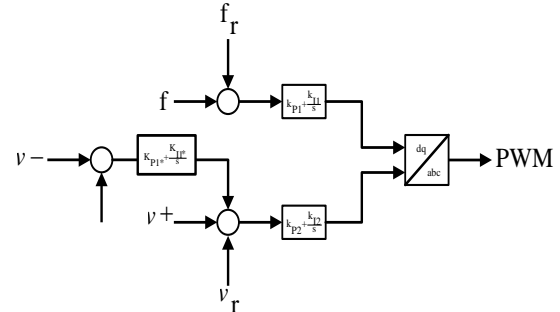

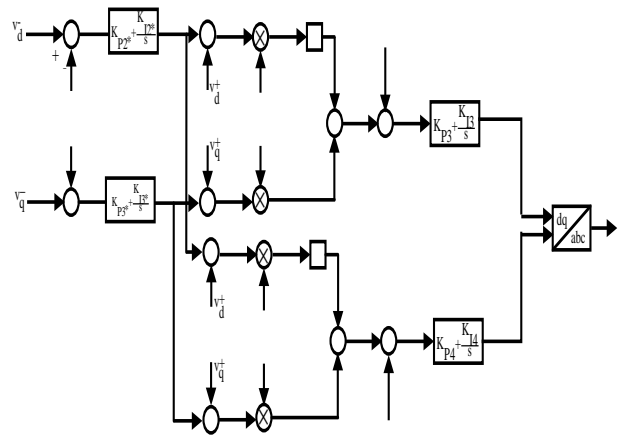**Figure 2.** Structure of the proposal control strategy for the frequency and voltage of the rotor.

Figure 3. Structure of the proposal control strategy for the power control of BESS.

Table 1. Test system parameters.

Asynchronous generator	Generator 1	$P_n = 275V\,A$ $V_n = 480\,V$ $f_n = 60\,Hz$
Transformers	Transformer 1	$\Delta\lambda - g, V_{1\,ph-ph}(V_{rms}) = 208\,V$ $R_{1(p.u.)} = 0.002, \qquad X_{1(p.u.)} = 0.04$ $(V_{rms}) = 480V, \qquad R_{2(p.u.)} = 0.002$ $V_{2\,ph-ph}(V_{rms}) = 480V, \qquad X_{2(p.u.)} = 0.04$
Transformers	Transformer 2	$\Delta\lambda - g, V_{1\,ph-ph}(V_{rms}) = 208\,V$ $R_{1(p.u.)} = 0.002, \qquad X_{1(p.u.)} = 0.04$ $(V_{rms}) = 480V, \qquad R_{2(p.u.)} = 0.002$ $V_{2\,ph-ph}(V_{rms}) = 480V, \qquad X_{2(p.u.)} = 0.04$
Loads	Load 1	$P_{load} = 10\,kW$
Wind turbine		Wind speed=15 m/sec

2.2. Objective function

The objective function of the proposed problem is introduced as Eq. (5), and it calculates the area under the curve following oscillations. In this problem, the objective function reveals the frequency oscillations and voltage, which should be minimized, but the frequency fluctuation has a greater effect than the voltage fluctuation on the power system stability. Hence, the under curve surface oscillations for the frequency are considered with a coefficient equal to 1.5. However, due to the significant relationship between oscillation of the active power and frequency under disturbances as well as the direct relation between the fluctuation of the reactive power and voltage magnitude, the fluctuations under the active power and reactive power oscillation curve can be added to the objective function.

$$\alpha \int_0^t t\left|\Delta f\right| \mathrm{dt} + \int_0^t t\left|\Delta V\right| \mathrm{dt} + \int_0^t t\left|\Delta P\right| \mathrm{dt} + \int_0^t t\left|\Delta Q\right| \mathrm{dt} \quad (5)$$

All the parameters of controllers are located between a maximum and minimum value which are listed in Table 2. This problem is solved by the ICA algorithm and its details can be explained in the next section.

3. ICA ALGORITHM

The ICA algorithm is a Multi-Factor algorithm simulating the social and political trend of imperialism and imperial competition. There are two types of country. The best countries are chosen as the "imperial state" and the remaining countries are the "colonies" of imperialists. Then, the colonies in the imperialists are divided according to their power. Any imperialism with its colony forms the "empire". The core processes of the ICA include the absorption and revolution within each empire, imperial competition among all empires, and the elimination of powerless empires. Under the policy of absorption, the colonies are moving in the empire of each respective imperialist side. Under the revolution policy, some of the colonies of each empire suddenly pass into other situations in each empire which are randomly selected. Under imperialist competition, a weak empire will lose its colony, so, its power gradually decreases and eventually fades away. All countries converge to an empire under the policy removal and so the algorithm stops.

The power of the entire empire depends on the power of both imperialist countries and their colonies. This fact is modeled by defining the power of the whole empire as an imperial power as well as the average power of its colonies [29]. The formulations of this algorithm are expressed as (6) to (10).

$$country = [p1, p2, p3, ...] \quad (6)$$

$$C_j = f_{\cos t}^{imp.j} - \max_i(f_{\cos t}^{imp.j}) \quad (7)$$

$$P_n = \left| \frac{C_n}{\sum_{i=1}^{N_{imp}} C_i} \right| \quad (8)$$

$$TC_j = f_{\cos t}^{(imp.j)} + \xi . \frac{\sum_{i=1}^{NC_j} f_{\cos t}^{(col.i)}}{NC_j} \quad (9)$$

$$P_j = \left| \frac{NTC_j}{\sum_{i=1}^{N_{imp}} NTC_i} \right| \quad (10)$$

Fig. 4 shows the flowchart for clarification of the proposed problem by the ICA algorithm. First, according to input data, the initial population is randomly generated (Eq. (6)). All the colonies of initial-population are distributed among the stated imperialists. The regularized cost of an imperialist is described by Eq. (7). The power of an empire is the inverse of the cost shown by Eq. (8). At that time, the colonies start to move toward their relevant imperialist country (Eq. (9)). The possession probability of each empire is expressed by Eq. (10). The weak empires will lose their power and they will finally collapse. The colonies move toward their relevant imperialists also, the collapse mechanism will cause all the countries to join to a state in which there exists just one empire and all the other countries are colonies belong to that empire. All the steps of this algorithm are showed in the flowchart of Fig. 4 [30].

Table 2. Parameters of PI controllers and stabilizers obtained using ICA algorithm.

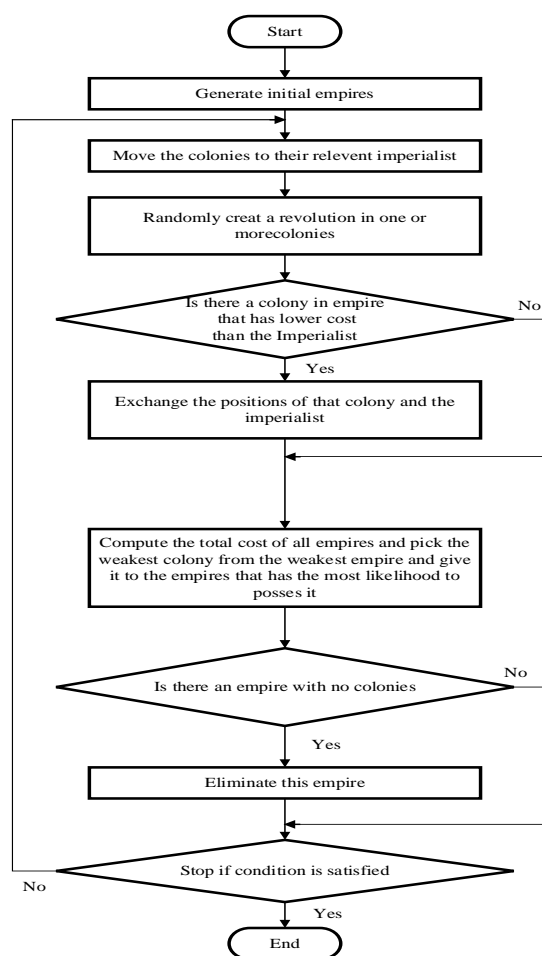|	Parameter	Minimum Value	Optimal Value	Maximum Value
Proportional Gains	K_{P1}	0.00001	0.00018	0.0005
	K_{P2}	0.0001	0.0002	0.0005
	K_{P3}	0.0001	0.00017	0.0005
	K_{P4}	0.00001	0.0001	0.0005
	K_{P1}^*	0.0001	0.00021	0.0005
	K_{P2}^*	0.0001	0.0001	0.0005
	K_{P3}^*	0.0001	0.0003	0.0005
Integral Gains	K_{I1}	0.01	0.2	0.5
	K_{I2}	0.01	0.1	0.5
	K_{I3}	0.01	0.21	0.5
	K_{I4}	0.01	0.34	0.5
	K_{I1}^*	0.01	0.11	0.5
	K_{I2}^*	0.01	0.14	0.5
	K_{I3}^*	0.01	0.23	0.5

Figure 4. Flowchart of the ICA algorithm.

4. SIMULATION RESULT

All the obtained simulation results are shown under balance and unbalance conditions with several scenarios including change the frequency reference with constant voltage, change the voltage reference with a constant frequency, application of the system with or without BESS, the operation of DFIG under On-Grid and Islanding mode.

4.1. Tuning of controllers

The parameters of the controllers have been tuned via the ICA algorithm, as the obtained results are listed in Table 2. It should be mentioned that the current problem was solved by various optimization techniques and the obtained results were compared to each other. Eventually, owing to the ICA finds the solution faster than the other techniques, it is selected to solve the problem. In order to confirm the reliability of the obtained simulation results, the setting of the algorithm was also changed, so, the problem was solved by the PSO algorithm. The value of the objective function of both algorithms is listed in Table 3. Table 2 is shown

the parameters of PI controllers and stabilizers obtained based on the ICA Algorithm.

Table 3. Objective function under different disturbances with PSO algorithm and ICA algorithm.

Algorithm	Objective function
ICA	198.2
PSO	256.41

4.2. Balance grid

4.2.1. Decoupled control of frequency and voltage regulation

In order to confirm the capability of the proposed strategy for voltage control subjected to the constant frequency, and also frequency control subjected to the constant voltage, under balance condition, the voltage setpoint is changed on 0.5 seconds and come back to the prior value on 2 seconds. The simulation results similar to these changes are shown in Figs. 5 and 6. It is clear that the voltage follows the alteration and also tracks the setpoint value, while the frequency drives back to the nominal value. Furthermore, the frequency follows the alteration and tracks the setpoint value of the reference despite the fact that the voltage drives back to the nominal value. As can be seen in Fig. 5, the maximum oscillation of the frequency is about 0.1 Hz during changing the voltage. While the magnitude of the voltage changes from 0.09 to 0.05 in 0.5 seconds and from 0.05 to 0.09 in 2 seconds. Fig. 6 shows the voltage oscillation magnitude between 0.085 and 0.095 during this fault. In this part, the simulation confirms that the voltage magnitude is constant after the frequency reference is set to 60.8 Hz from 60 Hz in 0.5 seconds and back to the 60 Hz in 2 seconds.
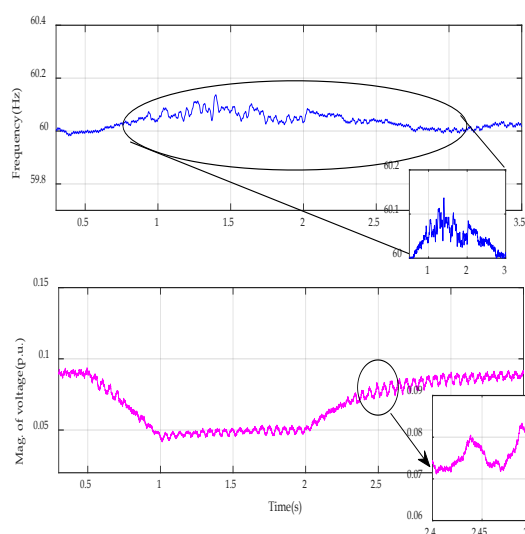

Figure 5. Frequency and voltage magnitude of the rotor after reference change of the voltage.
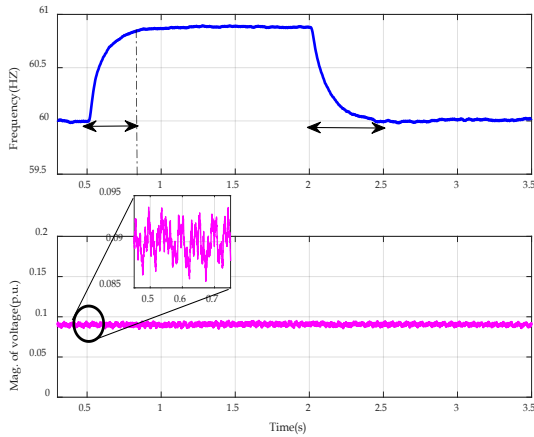
Figure 6. Frequency and magnitude of voltage of the rotor after reference change of the frequency.

4.2.2. Application of the system with BESS under both balance and unbalance conditions

In order to confirm the capability of BESS to supply the power injected to the grid, the active and reactive power of the load decreases and increases 20 % of nominal value. Although the active and reactive power is changed, however, the total active and reactive power is constant with a miniature oscillation.

Fig. 7 reveals that when the active and reactive power of load is modified, BESS supplies the required power. It means that by decreasing the consuming active power of the load, BESS produces less active power and by increasing reactive power, it's observed that this type of power is provided by BESS. Therefore, BESS can hold the entire power output constant. As a result, the productive active power decreases from -11 kw to -5 kw and reactive power changes from 8 kvar to -10 kvar.
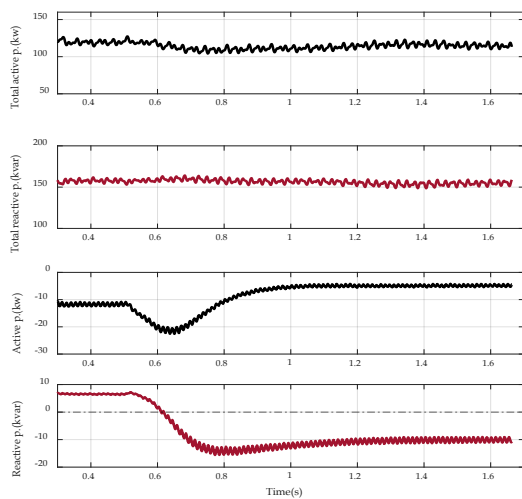

Figure 7. Total active and reactive power injected to the grid and the active and reactive power of BESS.
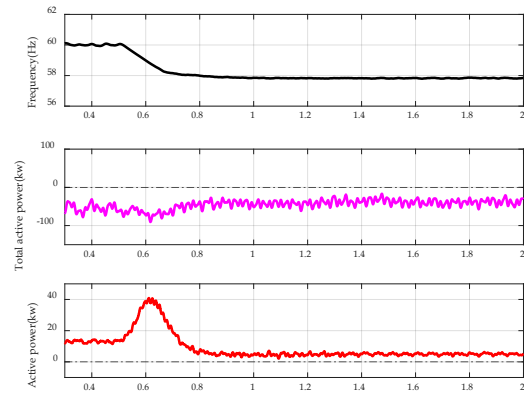

Figure 8. Total active power injected to the grid and the active and reactive power of BESS.

The unbalance condition in the simulation is a condition in which the voltage magnitude of each phase is different from each other. So, the simulation result is obtained under unbalance condition with employing BESS. Fig. 9 proves this hypothesis. Moreover, Fig. 8 confirms that if the frequency decreases from 60 Hz to 58 Hz, the active power of DFIG will decrease from 18 kw to 5 kw. In addition, the active power and total active of BESS is increased and fixed to the reference value, respectively, and BESS supplies the extra power. Fig. 9 shows a voltage magnitude is set to the user reference value after oscillation under the frequency pattern.

4.2.3. DFIG under islanding mode in balance and unbalance conditions

In this part, the result of the simulation is shown when DFIG operates under islanding mode under the balance condition. BESS can also supply the power of the load. The capacitive load is 15 kvar. As shown in Fig. 10, the active and reactive power of the load is set to be zero and -10 kvar, correspondingly. It is important to say that the distribution frequency and voltage magnitude go back to the reference value with oscillation.
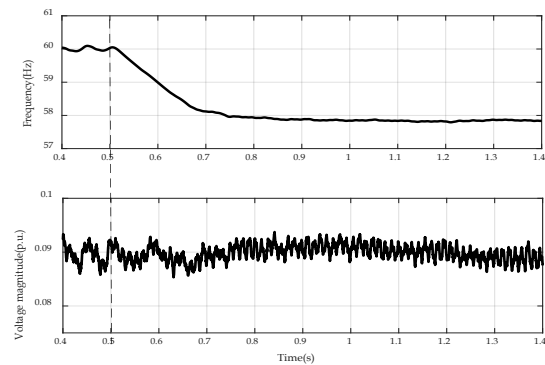

Figure 9. Frequency and voltage magnitude of the rotor and DC side voltage.
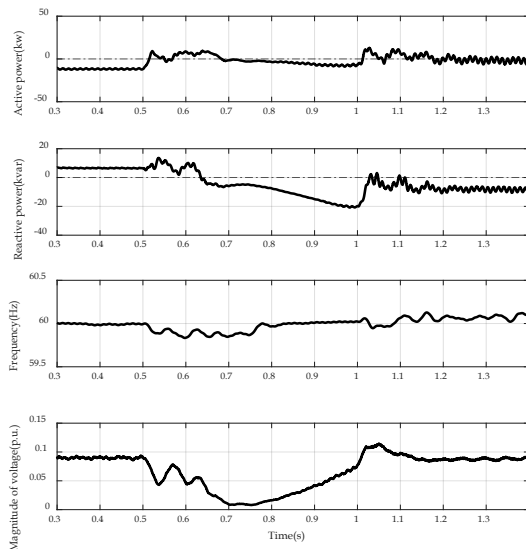
Figure 10. Total active and reactive power of load and frequency and magnitude of the voltage.
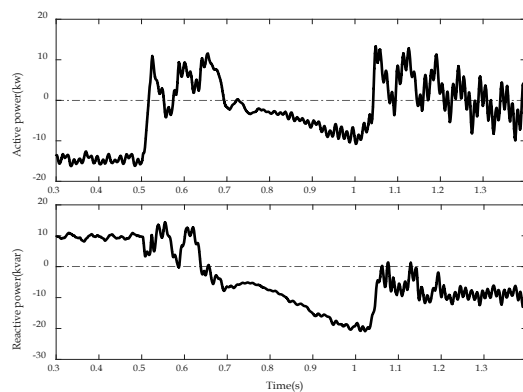

Figure 11. Total active and reactive power of the load.

In the next step, the capacitive load is 10 kvar. As can be seen in Fig. 11, when DFIG operates under the islanding mode based on the unbalance condition, the active power of the load is set to be zero and the reactive power is set to a negative value.

5. CONCLUSIONS

This paper focuses on improving the active and reactive power control of WECS by employing the BESS and controlling the frequency and voltage regulation instantaneously in balance, unbalance condition. Furthermore, an acceptable decoupling between the two components of both controllers was obtained. After an explanation of this suitable control, in order to study which condition has benefits for application of DFIG, a BESS was added to the system between the DFIG and the grid during voltage drop. In this paper, an unbalance control scheme is addressed for controlling the frequency, voltage and power control of BESS. According to the simulation results, the maximum

oscillation of the frequency is about 0.1 Hz during changing the voltage. Furthermore, the obtained simulation results confirm that the voltage magnitude is constant after setting the frequency reference to 60.8 Hz from 60 Hz in 0.5 seconds and back to the 60 Hz in 2 seconds. The BESS was installed on the system to supply the power of the load when DFIG operates under the islanding mode. All cases were explained in detail in the simulation result of this paper. In addition, the parameters of controllers were tuned by the intelligent algorithm to achieve the best result. By MATLAB simulation, this paper revealed the high dynamic performance obtained by proposed control. The proposed model is practical and presents low complexity and cost of implementation.

6. ACKNOWLEDGEMENT

REFERENCES

1. Ebrahimi, F.M., Khayatiyan, A. and Farjah, E., "A novel optimizing power control strategy for centralized wind farm control system", *Renewable Energy*, Vol. 86, (2016), 399–408.

2. Tahir, K., Belfedal, C., Allaoui, T., Denaï, M. and Doumi, M., "A new sliding mode control strategy for variable-speed wind turbine power maximization", *International Transaction on Electrical Energy Systems*, Vol. 28, No. 4, (2018), 3-25.

3. Mohseni, M. and Islam, S.M., "Review of international grid codes for wind power integration: Diversity, technology and a case for global standard", *Renewable and Sustainable Energy Reviews*, Vol. 16, No. 6, (2012), 3876–3890.

4. Jauch, C., Matevosyan, J., Ackermann, T. and Bolik, S., "International comparison of requirements for connection of wind turbines to power systems", *Wind Energy*, Vol. 8, No. 3, (2005), 295–306.

5. Shihabudheen, K.V., Krishnama Raju, S. and Pillai, G.N., "Control for grid-connected DFIG-based wind energy system using adaptive neuro-fuzzy technique", *International Transactions on Electrical Energy Systems*, Vol. 28, No. 5, (2018), e2526.

6. Delin, W., Ma, N., Gao, Y., Hu, Y. and Zhang, C., "Participation in primary frequency regulation of wind turbines using hybrid control method", *International Transactions on Electrical Energy Systems*, Vol. 28, No. 5, (2018), e2527.

7. Ameli, H., Abbasi, E., Ameli, M.T. and Strbac, G., "A fuzzy-logic–based control methodology for secure operation of a microgrid in interconnected and isolated modes", *International Transactions on Electrical Energy Systems*, Vol. 27, No. 11, (2017), e2389.

8. Persson, M. and Peiyuan, C., "Frequency control by variable speed wind turbines in islanded power systems with various generation mix", *IET Renewable Power Generation*, Vol. 11, No. 8, (2016), 1101-1109.

9. Heng, N., Cheng, P. and Zhu, Z.Q., "Independent operation of DFIG-based WECS using resonant feedback compensators under unbalanced grid voltage conditions", *IEEE Transactions on Power Electronics*, Vol. 30, No. 7, (2015), 3650-3661.

10. Tohidi, S. and Mohammadi-ivatloo, B., "A comprehensive review of low voltage ride through of doubly fed induction wind

generators", *Renewable and Sustainable Energy Reviews*, 57, (2016), 412-419.

11. Yateendra, M., Mishra, S., Li, F., Yang Dong, Z. and Bansal, R.C., "Small-signal stability analysis of a DFIG-based wind power system under different modes of operation", *IEEE Transactions on Energy Conversion*, Vol. 24, No. 4, (2009), 972-982.

12. Rahimi, M., "Drive train dynamics assessment and speed controller design in variable speed wind turbines", *Renewable Energy*, 89, (2016), 716-729.

13. Chen, G., Miao Hao, Z.X., Alun Vaughan, J.C. and Haitian, W., "Review of high voltage direct current cables", *CSEE Journal of Power and Energy Systems*, Vol. 1, No. 2, (2015), 9-21.

14. Liserre, M., Cardenas, R., Molinas, M. and Rodriguez, J., "Overview of multi-MW wind turbines and wind parks", *IEEE Transactions on Industrial Electronics*, Vol. 58, No. 4, (2011), 1081-1095.

15. Cardenas, R., Peña, R., Alepuz, S. and Asher, G., "Overview of control systems for the operation of DFIGs in wind energy applications", *IEEE Transactions on Industrial Electronics*, Vol. 60, No. 7, (2013), 2776-2798.

16. Morren, J., De Haan, S.W.H., Kling, W.L. and Ferreira, J.A., "Wind turbines emulating inertia and supporting primary frequency control", *IEEE Transactions on Power Systems*, Vol. 21, No. 1, (2006), 433-434.

17. De Almeida, R.G. and Peças Lopes, J.A., "Participation of doubly fed induction wind generators in system frequency regulation", *IEEE transactions on Power Systems*, Vol. 22, No. 3, (2007), 944-950.

18. Moutis, P., "Discussion on "Primary Frequency Regulation by Deloaded Wind Turbines Using Variable Droop"", *IEEE Transactions on Power Systems*, Vol. 29, No. 1, (2014), 414-422.

19. Fazeli, M., Asher, G.M., Klumpner, C., Yao, L. and Bazargan, M., "Novel integration of wind generator-energy storage systems within microgrids", *IEEE Trans. Smart Grid*, Vol. 3, No. 2, (2012), 728-737.

20. Shuo, W., Hu, J. and Yuan, X., "Virtual synchronous control for grid-connected DFIG-based wind turbines", *IEEE Journal of Emerging and Selected Topics in Power Electronics*, Vol. 3, No. 4, (2015), 932-944.

21. Yan, X., Venkataramanan, G. and Wang, Y., "Grid-fault tolerant operation of DFIG wind turbine generator using a passive resistance network" *In Energy Conversion Congress and Exposition*, (2009), 382-389.

22. Mohammadi, J., Afsharnia, S., Vaez-Zadeh, S. and Farhangi, S., "Improved fault ride through strategy for doubly fed induction generator based wind turbines under both symmetrical and asymmetrical grid faults", *IET Renewable Power Generation*, Vol. 10, No. 8, (2016), 1114-1122.

23. Tohidi, S., Oraee, H., Zolghadri, M.R., Shao, S. and Tavner, P., "Analysis and enhancement of low-voltage ride-through capability of brushless doubly fed induction generator", *IEEE Transactions on Industrial Electronics*, Vol. 60, No. 3, (2013), 1146-1155.

24. Vidal, J., Abad, G., Arza, J. and Aurtenechea, S., "Single-phase DC crowbar topologies for low voltage ride through fulfillment of high-power doubly fed induction generator-based wind turbines", *IEEE Transactions on Energy Conversion*, Vol. 28, No. 3, (2013), 768-781.

25. Hemmati, R. and Azizi, N., "Optimal control strategy on battery storage systems for decoupled active-reactive power control and damping oscillations", *Journal of Energy Storage*, Vol. 13, (2017), 24-34.

26. Hemmati, R., and Azizi, N., "Nonlinear modeling and simulation of battery energy storage systems incorporating multiband stabilizers tuned by Meta-heuristic algorithm", *Simulation Modelling Practice and Theory*, Vol. 77, (2017), 212-227.

27. Kai, L., He, Z., Wang, Y. and Yang, J., "An input–output linearization algorithm-based inter-area damping control strategy for DFIG", *IEEJ Transactions on Electrical and Electronic Engineering*, Vol. 13, No. 1, (2018), 32-37.

28. Khazaeli Moghadam, F., Ebrahimi, S.M., Oraee, A. and Mohammadpour Velni, J., "Vector control optimization of DFIGs under unbalanced conditions", *International Transactions on Electrical Energy Systems*, (2018), e2583.

29. Azari Niaz, M., Mirsalim, M., Abedi Pahnehkolaei, S.M. and Mohammadi, S., "Optimum design of a line-start permanent-magnet motor with slotted solid rotor using neural network and imperialist competitive algorithm", *IET Electric Power Applications*, Vol. 11, No. 1, (2017), 1-8.

30. Rahmani, R. and Fakharian, A., "New control method of islanded microgrid system: A GA & ICA based optimization approach", *The Modares Journal of Electrical Engineering*, Vol. 12, No. 4, (2016), 40-49.